Supporting Information

Angel et al. 10.1073/pnas.1503100112

SI Text

Full Model

To simulate in detail the transfer of nucleation to *cis*-acting silencing memory via histone modifications, we used a slightly modified version of the model previously applied to the vernalization system (1). The core of the model is nearly identical to that presented in ref. 1. Our original parameterization was used as a starting point for our fitting, with many parameters remaining unchanged; details are in Table S1. We provide an additional description of the simulation here for clarity and ease of reproduction and refer the reader to the main text for a description with greater detail.

The core model of histone-based epigenetic memory is centered on the assumption that there are two main types of opposing histone modification that activate or silence the system, called M (for H3K27me3, a silencing modification) and A (for an activating modification). In addition to this, there is a U state (for unmodified) that describes the absence of both modifications on a particular histone. The system is modeled as a stochastic process where events are given specific probabilities per unit time of occurring. The central mechanism that allows for stable epigenetic memory is long-range cooperative positive feedback. The M modifications tend to recruit more M modifications and remove A modifications; similarly, the A modifications tend to recruit more A modifications and remove M modifications. Moreover, the recruitment/removal processes can occur between two histones that are spatially far apart through, for example, gene looping. With this core mechanism in place the system is capable of maintaining itself in a state in which a clear majority of histones have the A modification, giving an active locus, or the M modification, giving a silenced locus.

This study focuses on the way that the system switches from an activated to a silenced state. This switch can be triggered by the nucleation of a given histone modification in a localized region of the *FLC* gene—referred to as the nucleation region. A small bias in one direction is also added postcold to help the nucleated signal enforce a switch of states. This is motivated biologically by a postcold increase in the activity of the enzymes that add M modifications and remove A modifications, for example, via the transient activity of the plant homeodomain (PHD) protein VRN5. Neither of the processes of nucleation and bias on their own are enough to cause switching within a short period, but the combination of the two is very effective at causing a switch between active and silenced states. The persistence of nucleation and bias is modeled as limited duration events in the warm period directly following cold exposure.

The system comprises $L = 70$ modifiable histones (the equivalent of 35 nucleosomes, with 2 copies of the histone able to accept the relevant modifications per nucleosome). The histones themselves are divided into those that are in the nucleation region, taken to be 5 histones in extent (1), and those that are outside (the body region), with different rules for each. As mentioned above, we impose long-range interactions such that any histone can communicate equally efficiently with any other within the locus. Hence, other than the distinction between the nucleation and body regions, the actual position of the nucleation region at *FLC* is unimportant. Time is divided into steps equivalent to 15 s in real time, so that there are 5,760 time steps in a single day. Certain parameters take different values at different times during the simulation to model the effect of, for example, different temperatures—in the bulleted list below, these are denoted by subscripts of the appropriate parameters and are detailed in Table S1.

In each time step, there are a number of updates equal to the number of histones. In each update, a histone is chosen at random. Probabilities are assigned to each possible event, dependent on the state of the system at a given time. A random number is then generated and used to select an event with a likelihood proportional to its probability.

For histones outside the nucleation region, where N_M is the total number of histones in the M state and N_A is the number histones in the A state, we have the following:

- With probability $\mu\alpha N_M/L$, a histone in the A state will be changed to the U state.
- With probability $\mu\alpha N_M/L + \gamma/2$, a histone in the U state will be changed to the M state.
- With probability $\alpha N_A/L + \gamma/2$, a histone in the U state will be changed to the A state.
- With probability $\alpha N_A/L$, a histone in the M state will be changed to the U state.
- With probability β, the histone and its neighboring histone in the same nucleosome will have any modifications removed, i.e., be set to the U state. This process models spontaneous nucleosome swap out.

For histones inside the nucleation region, we have the following:

- With probability $\eta\mu\alpha N_M/L$, a histone in the A state will be changed to the U state.
- With probability $\eta\mu\alpha N_M/L + \gamma/2 + \omega + \theta(t)\epsilon$, a histone in the U state will be changed to the M state.
- With probability $\omega + \theta(t)\epsilon$, a histone in the A state will be changed to the M state.
- With probability $\eta\alpha N_A/L + \gamma/2$, a histone in the U state will be changed to the A state.
- With probability $\eta\alpha N_A/L$, a histone in the M state will be changed to the U state.
- With probability β, the histone and its neighboring histone in the same nucleosome will have any modifications removed, i.e., be set to the U state.

As a separate event, once a day in warm conditions and once a week in cold conditions, the effect of DNA replication was included in the simulations. During this event, with probability p_{rep}, each nucleosome has both of its histones set to the U state. As initial conditions, a fraction of simulated cells were placed in a fully silenced state, completely covered with M modifications. Table S1 has a full list of the parameters and their values.

As stated above, some of the parameters take on different values, depending on the time in the simulation. The bias parameter, μ, takes on the value μ_1 before and during cold. In a period of warm directly following a period of cold, the bias parameter takes on the value μ_2 for a period t_b, before reverting back to μ_1. For the analog model the nucleation parameter, $\theta(t)$, is allowed to build up during the cold in all cells and remains at the same level in the following time period t_n, before taking on a value of 0. In the class 1 digital model, the nucleation parameter switches from 0 to 1, with a probability that builds up during the cold. The nucleation parameter then remains at the same level in the following warm time period t_n, before taking on a value of 0. In the class 2 digital model, the nucleation parameter can switch dynamically between values of 0 and 1 during

the cold and in the period directly following cold, with the fraction of time spent with value 1 increasing as a function of cold exposure duration, before taking on a permanent value of 0 a time t_n after the end of cold exposure. Unless otherwise stated, all simulations had a period of 1 wk in the warm before any cold was applied. We next describe in detail how the nucleation parameter builds up and behaves in a different fashion for the analog and digital models.

New Rules for the Buildup of the Nucleation Peak

The only differences between the analog and digital models (other than potentially different parameter values) lie in the dynamics of the nucleation peak buildup and persistence during and at the end of cold exposure. To have the analog and digital models functioning on a similar footing to each other, it was desirable to have similar forms for the buildup of the nucleation peak. Similar to our previous approach (1), a Hill function was chosen, due to its simple functional form and excellent fit to the data. Without more insight into the upstream processes causing nucleation, it is not possible to be more specific about how such a profile is generated mechanistically. In the analog model, during the cold, the nucleation parameter, $\theta(t)$, builds up according to the Hill function $Ct_w^h/(K+t_w^h)$, where t_w is the time in cold measured in weeks, and C, h, and K are parameters. In the class 1 digital model, generating such a Hill function is more complex. At each time step of the simulation during cold exposure a cell becomes competent to nucleate; i.e., the parameter $\theta(t)$ makes a transition from 0 to 1, with a probability $p(t_w)$ equal to

$$p(t_w) = Cht_w^{h-1}\frac{1-t_w^h/(K+t_w^h)}{T_w(K+(1-C)t_w^h)},$$

where T_w is the number of time steps in the simulation equivalent to 1 wk in real time. This probability is designed to give a Hill function form for the level of the peak. In the digital class 1 model, cells switch to a nucleating state with a given probability per unit time but the number of cells that have already switched will affect the overall rate of further switching. This can be described by the equation $dS(t_w)/dt_w = (1-S(t_w))p(t_w)T_w$, where $S(t_w)$ is the fraction of cells that have switched up to time t_w. The above form for the probability is chosen such that the solution to the fraction of cells that switch is a Hill function, as chosen for the analog model. In the class 2 digital model, $\theta(t)$ switches between 0 and 1 dynamically, with the probability at each time step at which it switches to the nucleating state (0 to 1) increasing with cold exposure duration according to $\theta_{on} = \theta_{on,max} \times Ct_w^h/(K+t_w^h)$. The probability at each time step at which it switches out of the nucleating state (1 to 0) is fixed at θ_{off}. Note that the parameters C, h, and K are allowed to differ between the analog and digital models.

Measuring Histone Modification and Spliced mRNA Levels from Simulations

Results from the simulations are given in terms of the occupancy of histone modifications of a given type, expressed as a fraction of the maximum possible levels, when the system is entirely populated with that modification. The simulated M modification (H3K27me3) levels shown in Fig. 2*A* are averaged over all cells for 1 d up to the corresponding time point on the x axes.

Many of our results are measured as spliced mRNA levels relative to the nonvernalized level. To determine the relative expression from our simulations we assume that the relative reduction in expression is equal to $(1-S_e)/(1-S_b)$, where S_e is the fraction of cells that are silenced at the end of the simulation and S_b is the fraction of cells that are silenced at the beginning of the simulation. A cell is counted as silenced if its average silencing histone modification occupancy in the *FLC* gene body is greater than 0.5, all averaged over the initial 5 d of a simulation (for S_b) or the 5 d following the 7th d after the final cold exposure (for S_e). The precise value of 0.5 is unimportant as identical results were found for values of 0.4 and 0.6.

Parameterization of the Models

The models were parameterized using a mixture of experimental ChIP and expression data. ChIP data in the nucleation region immediately after cold and after a 7-d warm period following cold and relative expression data after a 7-d warm period following cold—all NV, 2 wk, 4 wk, 6 wk, and 8 wk of uninterrupted cold—were used for the fitting. For the ChIP, simulated M levels were compared with experiments on the assumption that the maximum possible experimental level, where we plot (H3K27me3 *FLC*/H3 *FLC*)/(H3K27me3 *STM*/H3 *STM*), is one. This is a reasonable working assumption as *STM* is silenced in almost all cells in a plant and should be accordingly highly methylated. Best fits were chosen such that as many points as possible satisfied one-tailed t tests (at the 5% confidence limit), treating the simulation data as having effectively zero variance. The class 1 digital model satisfied this test at all points, whereas the class 2 digital and analog models failed at the 4-wk cold plus 7-d warm period for the ChIP and at the 2-wk cold plus 7-d warm period for the expression, as discussed in the main text.

Generation of the Probability that a Cell Switches to the Silenced State

We used our simulations to analyze the form of the switching probability for the analog model (Fig. 3*A*). Using our best-fit parameter set, runs were performed for 10^5 realizations (equivalent to individual cells) for values of the nucleation parameter, ϵ, ranging from 0 to 0.6 in increments of 0.005—thus generating 121 different levels of nucleation. Simulations were run for an initial period of 5,760 time steps (the equivalent of a single day), with a precold/during cold value for the bias parameter and nucleation in effect. From this initial part of the simulation, the level of the H3K27me3 nucleation peak was extracted (averaged over the full time of this initial period and over the population of simulated cells). Following this (and as in simulations for the full model), simulations were continued for a period of 23,040 time steps (the equivalent of 4 d) with nucleation and a postcold value for the bias parameter and then for a further 17,280 time steps (3 d) with nucleation but a precold value for the bias (i.e., no further aid to spreading). After this, the simulations were continued without nucleation for a further two periods of 5,760 time steps. For each run, the level of M modifications was then averaged in the body region separately for the further two periods. Cells were judged to have successfully spread if the average M level in the body was greater than 0.5 of the maximum possible for both of these final periods (again the precise value of 0.5 was unimportant; using 0.4 or 0.6 generated identical results). A nearly identical procedure was followed for the digital models for later use in comparing the models. The only difference for the digital class 1 model was that the fraction of nucleating cells was varied from 0 to 1 in increments of 0.008. The only difference for the digital class 2 model was that the probability at each time step at which individual cells switch to the nucleating state was varied from 2.5×10^{-5} to 0.1 in varying increments (but most commonly 0.001). The probability at each time step at which individual cells lose the nucleation peak was left unaltered.

Initial Presilencing, Weak Nucleation, and Nucleation Region Feedback Are Not Essential for Our Conclusions

Experimental observations indicate that in the *Columbia* line *FRI*-Sf2, there are low but still significant levels of H3K27me3 at *FLC* even before a plant has experienced any cold. There is also compelling evidence that H3K27me3 levels are higher in the nucleation region than at the rest of the locus, as seen in our

ChIP data and ref. 1. To capture this finding in our full model, a fraction of the cells were started in a fully silenced state (Table S1). Furthermore, at all times and in all cells, a small amount of nucleation was added as well as feedback from outside the nucleation region into the nucleation region, with parameters ω and η, respectively, as described above. These additions were needed to produce good model fits but were otherwise unimportant to the core mechanisms involved. To ensure that these effects were not responsible for the differences between the analog and digital models, we removed them, i.e., set $\omega = 0$ and $\eta = 1$. We found that the switching probability in the analog model retains its shape and is practically identical to the full model result shown in Fig. 3*A*, with nonlinearity particularly noticeable for low and high nucleation levels. For this reason, the deficiency of the analog model in responding to short periods of cold exposure is retained. This change when applied to the digital models similarly has no effect on the shape of the switching probability.

Functional Form of the Nucleation Peak Buildup That Would Be Required for the Analog Model to Match the Digital Class 1 Model

We also performed an analysis of the functional form for the nucleation peak buildup that would be required to make the analog model perform equally well to the digital class 1 model with respect to the expression data. This involves taking the digital class 1 nucleation peak values during the cold and first computing the corresponding fraction of cells that are nucleating (but not presilenced). From this fraction, we can then work out the resulting digital silencing. Next, we can use the analog switching probability data to work out the analog peak value required to give an equivalent level of silencing. Finally, this value can be combined with the fraction of presilenced cells to generate a final peak value that can be compared directly with the experimentally measured nucleation peak.

The starting point is the digital class 1 model fitted to the experimental nucleation peak values (Fig. 2*A*). This nucleation peak value is generated by silenced cells, nonsilenced cells that are in the nucleating state, and nonsilenced cells that are not in the nucleating state. The average nonnucleating, nonsilenced peak height (nnnsc) was taken from the first day of the switching simulation (see above) with no cells in the nucleating state. The average nucleating, nonsilenced peak height (nnsc) was also taken from the first day of the switching simulation, but now with all cells in the nucleating state. The average silenced peak height (sc) was taken from the final day of the switching probability simulation with all cells having been previously placed in the nucleating state. The peak height at any given time should thus correspond to $\mathrm{dig}_{\mathrm{T0}} = \mathrm{dig}_{\mathrm{sil}} \times \mathrm{sc} + (1 - \mathrm{dig}_{\mathrm{sil}} - \mathrm{dig}_{\mathrm{nuc}}) \times \mathrm{nnnsc} + \mathrm{dig}_{\mathrm{nuc}} \times \mathrm{nnsc}$, where $\mathrm{dig}_{\mathrm{T0}}$ is the average H3K27me3 level in the nucleation region for the digital class 1 model at a given time, $\mathrm{dig}_{\mathrm{sil}}$ is the fraction of cells that are silenced, and $\mathrm{dig}_{\mathrm{nuc}}$ is the fraction of cells that are nucleating but nonsilenced at a given time. The above formula is used to extract the fraction of cells $\mathrm{dig}_{\mathrm{nuc}}$ that are nucleating but nonsilenced immediately at the end of cold treatment, from 0 wk to 8 wk in increments of 1 d in the digital class 1 simulation. The fraction of cells that would silence for each length of cold is then calculated by multiplying the fraction of nucleating cells by the switching probability (0.98 for our chosen parameters).

The computed switching probability for the analog model (collected as described in a previous section) is composed of a number of sampled nucleation peak levels together with the corresponding fraction of cells that switch. This can be inverted and interpolated (using linear interpolation as there are many closely spaced samples) to give a function for the nucleation peak level required to produce a given level of silencing. This function was used to compute the analog peak height required to give the same fraction of cells silenced by each period of cold treatment (from 0 wk to 8 wk in increments of 1 d) as in the digital class 1 model. However, this peak height does not include the fraction of presilenced cells of the full model, so the full required analog peak height is reconstructed using the formula $\mathrm{ana}_{\mathrm{T0}} = \mathrm{ana}_{\mathrm{sil}} \times \mathrm{sca} + (1 - \mathrm{ana}_{\mathrm{sil}}) \times \mathrm{ana}_{\mathrm{pk}}$. Here $\mathrm{ana}_{\mathrm{pk}}$ is the nucleation peak height that is required to give the same fraction of silenced cells postcold as for the digital class 1 model as calculated above, $\mathrm{ana}_{\mathrm{sil}}$ is the fraction of presilenced cells in the analog model, and sca is the average nucleation peak level for silenced cells in the analog model. Note that the initial fraction of silenced cells is the same in the analog and digital models.

Linking the Conceptual and Histone Modification-Based Models

In the main text, we presented a simple conceptual model for cold-induced switching and epigenetic memory. In this section, we link it more closely to our specific histone modification-based model.

We consider a variable, x, that represents the expression state of the system. Around $x = -1$, the system is in a high expression state, whereas around $x = 1$ expression of the gene is silenced. We assume that each of these two states is stable and therefore that there exists a potential landscape that pushes the system toward one of the two stable states, as illustrated in Fig. 5. This potential landscape can be naturally interpreted in the specific case of a histone-based epigenetic memory system, as we now describe. Around $x = -1$, the gene is mostly occupied by activating A modifications, whereas around $x = 1$, the system is mostly occupied by silencing M modifications. The neutral state around $x = 0$ represents a roughly equal mixture of M and A modifications, with the remainder of histones (if any) being unmodified. Neglecting any biases, when $x < 0$, with a greater number of A than M modifications, the system will tend to relax toward $x = -1$ due to its intrinsic positive feedback. When $x > 0$, with a greater number of M than A modifications, the system will tend to relax toward $x = 1$. Thus, there is a threshold that divides the two stable states of the system. This dynamic positive feedback can be viewed as a potential landscape that pushes the system back to one of the two stable expression steady states. However, as we emphasized in the main text, this potential representation is actually more general than the histone-based modification system, as it can in principle describe any system with stable steady states without specifying in detail what mechanism stabilizes the steady states.

In terms of a histone-modification–based model, the single variable x represents both the expression state of the gene and the relative levels of M vs. A modifications. However, at *FLC* the cold-induced H3K27me3 nucleation peak is potentially present only over a limited number of nucleosomes, not over the entire locus. Hence, as we now describe, at the end of cold exposure x will be lower than previously assumed, to account for the lower levels of population-level H3K27me3.

Before cold exposure, the system is in a state close to $x = -1$ and the entire distribution around this value is below the threshold at $x = 0$. At the end of cold exposure, population-level H3K27me3 has increased but only in the spatially limited nucleation region. In the analog model, this corresponds to an increased value for x that is approximately equal in all cells and is higher after a longer duration of cold exposure. In the digital class 1 model, this corresponds to an increasing fraction of cells having gained a fixed jump in the value of x. However, even in the digital class 1 case, due to the limited nucleation region, it is likely that the value of x reached after such a jump is still not sufficient deterministically to push the system over the potential "peak" threshold separating the two stable states, allowing the system state to be switched. Here two additional factors are important. First, the system is not entirely deterministic but rather the value of x is actually drawn from a distribution. Therefore, if the peak

is maintained for some time following cold exposure [as is known to be the case experimentally (1)], there is time for the system to explore values away from its deterministic value and eventually acquire a value that is large enough to generate a switch. Second, the full model includes a temporary bias toward the M modification (the equivalent of increasing the rate of nonnoisy interactions toward the M state). This effect is like altering the potential and shifting the threshold such that a smaller deviation from $x = -1$ is required to allow a switch of the system from the active to the silenced state.

Importantly, despite the above changes, the differences between the digital class 1 and analog mechanisms are still present. For the digital class 1 mechanism, in an individual cell after a jump, the portion of the distribution past the threshold is always the same irrespective of the length of cold treatment and so can still give a high probability of switching. The number of cells that switch will therefore still be in direct proportion to the number of cells that have digitally acquired nucleation. For the analog mechanism, the portion of the distribution past the threshold will be approximately equal in all cells. Except in the case of a uniform distribution around the deterministic value of x (which would be an extremely unusual configuration), the switching probability will be nonlinear with the level of nucleation. Thus, the analog mechanism suffers from the same problem as before—a nonlinear increase in the switching probability with the height of the nucleation peak, with inappropriately low switching for smaller peaks.

Perfect Buffering of Interrupted Cold: Exponential Approach to Saturation

In the main text, we showed that there is a form for the population-level digital nucleation peak buildup in the digital class 1 model that would provide perfect buffering of any number of interruptions. We now allow for a fraction of cells silenced before cold exposure, as well as for a small nucleation peak in cells that have not responded to cold exposure. We therefore fit the function $c_0 - c_1 \exp(-c_2 t)$, where c_0, c_1, and c_2 are the fit parameters, to the nucleation peak profile as measured at the end of uninterrupted cold periods of 0 wk, 2 wk, 4 wk, 6 wk, and 8 wk and also to the corresponding spliced *FLC* mRNA levels relative to no cold treatment. This was done by minimizing the χ^2 test statistic between the above function and the ChIP data points for the nucleation peak and between $\exp(-c_2 t)$ and the mRNA data points for the relative mRNA levels (combining the two for a single test statistic). The resulting fits are shown in Fig. S1.

Pooling of Experimental Data

For the parameterization of the model, experimental data were collected in the form of ChIP of H3K27me3 in the nucleation region and relative expression of *FLC*. ChIP data were also collected for the "body" region of the gene but were not used for fitting. These data were collected over an extended period and were pooled together. The ChIP data were collected in three batches of experiments. One of these (batch JQ, Table S2) had less coverage of the body region and was therefore used only for the nucleation region. For each batch, the nucleation and body regions were defined and four primer sets in the nucleation region and five in the body were averaged over. The details of the primers used for each batch can be found in Table S2. For two of the batches, labeled JS and HY, data were collected before and immediately after cold and after cold plus a period of 7 d of warm (NV, T0, and T7). For one of the batches, labeled JQ, the data collected after cold plus a period of warm were taken following a period of 10 d of warm. The models (and a comparison between the experimental levels in the different batches) indicated that there were no significant differences between these time points. Hence, these data points were treated as T7 data and pooled with the others. Similarly, expression data were collected alongside the ChIP experiments for uninterrupted cold, with some collected at 7 d after cold and some at 10 d after cold. These data were again pooled. Additional expression datasets were collected for the interrupted and uninterrupted cold comparison, with the postcold warm period varied in the uninterrupted sets to match the total warm in the interrupted sets. For the purposes of comparing the uninterrupted and interrupted cold, these data were treated separately. However, for model parameterization, the uninterrupted postcold plus warm expression levels were pooled and treated as T7 data as before. The number of samples collected in each batch is detailed in Table S3. For relative expression measurements, spliced *FLC* mRNA was measured relative to NV levels. NV refers to samples that were not exposed to cold (nonvernalized). For uninterrupted cold, NV samples were taken with 14 d total growth in the warm condition with the exception of the JQ batch for which samples were taken with 10 d total growth in the warm condition. For the interrupted case, for two and three interruptions, NV samples were taken with 18 d total growth in the warm condition (except for one batch taken with 22 d total growth in the warm condition). For a single interruption, NV samples were taken with 14 d total growth in the warm condition.

Calculation of Errors

For the ChIP data, errors presented are the SEM for measurements from ref. 1 and further biological replicates previously unpublished. For experimental expression values, technical replicates for each time point (including the nonvernalized samples) were averaged and this average was treated as an independent sample. The ratio of this value for each time point was taken with the nonvernalized sample for the same experiment. These relative values were then taken as our biological replicate measurements and errors given as the SEM over the biological replicates. For our simulations, the histone modification occupancy measurements were taken to be the average level of M modifications in a given region over a period of 1 d. Errors on this quantity were found as the SEM over all independent simulation realizations. For the computed *FLC* expression levels from the models, 10 simulations of 1,000 realizations were run, where each simulation was treated as an independent sample for the fraction of cells silenced, with the error taken as the SEM over these samples. In all cases these initial errors were propagated through any further processing/calculation steps, using the standard formula for propagation of errors. The sizes of the resulting relative errors for the histone modification levels were very small, on the order of 10^{-3}, and are not shown in the figures.

1. Angel A, Song J, Dean C, Howard M (2011) A Polycomb-based switch underlying quantitative epigenetic memory. *Nature* 476(7358):105–108.

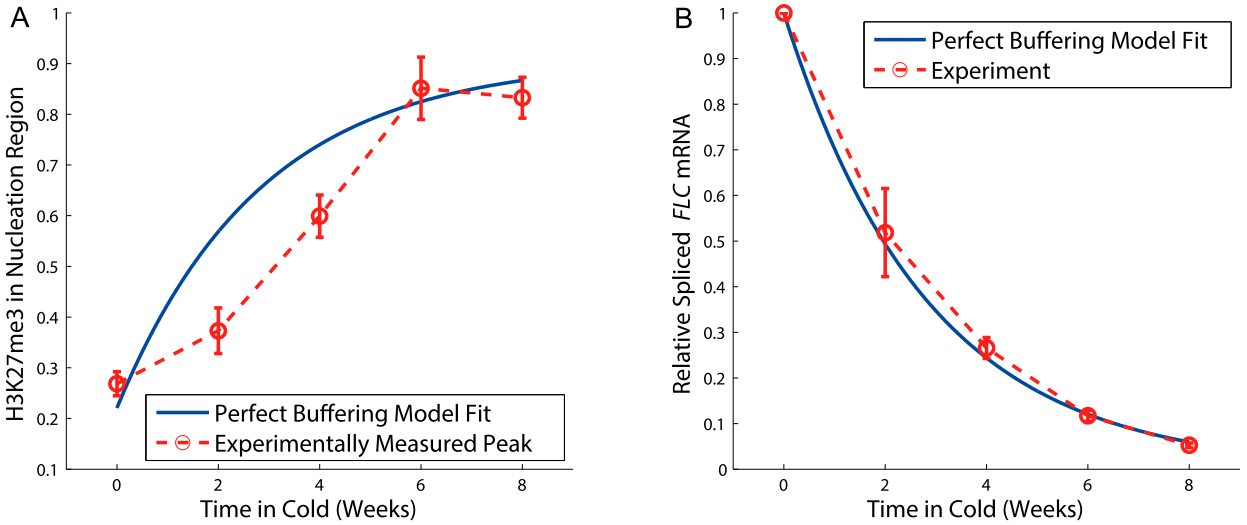

Fig. S1. (*A*) Experimentally measured H3K27me3 nucleation peak profile as a function of cold exposure duration (red dashed line and data points, as in Fig. 2). Blue line is simulated, population-averaged, H3K27me3 nucleation peak profile from digital class 1 model required to perfectly buffer cold interruptions (fitted to the H3K27me3 level in the nucleation region and relative expression levels). (*B*) Experimentally measured expression profile following uninterrupted cold (red dashed line and data points, as in Fig. 2). Blue line is the relative expression level from the same simulation as in *A*.

Table S1. Parameters and their descriptions used in the analog and digital models, together with best-fit values where appropriate

Parameter/variable	Description	Digital class 1 model value	Digital class 2 model value	Analog model value
L	Number of histones in system	70	Same	Same
Time step	Length of time represented by each time step in simulation	15 s	Same	Same
DNA replication	Frequency with which system undergoes DNA replication	1/d (warm), 1/wk (cold)	Same	Same
μ	Bias in transitions A to U and U to M	Variable (see below)	Same	Same
μ_1	Bias before and during cold and after period t_b following end of cold	0.9	Same	Same
μ_2	Bias during period t_b following end of cold	1.1	Same	Same
α	Factor controlling modification of addition/removal probability per time step due to other modifications	0.05	Same	Same
N_M	Number of histones with M modification at given time	Variable	Same	Same
N_A	Number of histones with A modification at given time	Variable	Same	Same
γ	Additive probability per time step with which random modification is added to unmodified histone	0.002 (refitted)	Same	Same
β	Probability per time step with which nucleosome is replaced by unmodified one	0.0025	Same	Same
η	Multiplicative factor modulating probability of modification change in nucleation region due to other modifications	4.0	Same	Same
ω	Additive probability with which histone is changed to M state in nucleation region (weak nucleation)	0.035	Same	Same
$\theta(t)$	Multiplicative factor modulating probability of cold-induced nucleation event	Allowed to take value 0 or 1 in individual cells	Same, but switches back and forth between 0 and 1 dynamically	Allowed to vary smoothly from 0 to 1 in individual cells
θ_{on}	Probability per time step that a cell switches into the nucleating state (during cold and postcold in the class 2 digital model)	N/A	Variable—depends on cold exposure	N/A
$\theta_{on,max}$	Maximum possible value of θ_{on}	N/A	0.075	N/A
θ_{off}	Probability per time step that a cell switches out of the nucleating state (during cold and postcold in the class 2 digital model)	N/A	0.006	N/A
ϵ	Multiplicative factor for probability per time step of histone in nucleation region being changed to M state as result of cold exposure	0.6	Same	Same
p_{rep}	Probability per time step that nucleosome is replaced with unmodified one during DNA replication	0.5	Same	Same
t	Time in cold, measured from start of latest cold period	Variable	Same	Same
t_b	Number of time steps for which bias is increased postcold while in warm	23,040 (refitted)	Same	Same
t_n	Number of time steps for which nucleation remains postcold while in warm	40,320 (refitted)	Same	Same
t_w	Number of time steps in 1 wk of real time	40,320	Same	Same
C	Constant of proportionality of the Hill function	1.025	1.0	1.0
h	Hill coefficient	2.35	3.0	2.2
K	Effective dissociation constant of the Hill function	10.0	325.0	30.0
M_s	Probability with which individual cells are placed in fully silenced state at beginning of simulation	0.07	0.09	0.07

Those parameters whose values have altered from previously published fits (γ, t_b, t_n) are indicated in the Digital class 1 model value column. N/A indicates that the variable or parameter is not applicable to the corresponding version of the model.

Table S2. Details of the ChIP primers used in the different experiment batches

Batch	Nucleation region primers	Nucleation region primer sequence 5′–3′	Gene body region primers	Gene body region primer sequence 5′–3′
JS	48_F	CGACAAGTCACCTTCTCCAAA	3,088_F	GGGGCTGCGTTTACATTTTA
	205_R	AGGGGGAACAAATGAAAACC	3,224_R	GTGATAGCGCTGGCTTTGAT
	307_F	GGCGGATCTCTTGTTGTTTC	3,899_F	CTTTTTCATGGGCAGGATCA
	393_R	CTTCTTCACGACATTGTTCTTCC	4,069_R	TGACATTTGATCCCACAAGC
	679_F	TCATTGGATCTCTCGGATTTG	4,213_F	AGAACAACCGTGCTGCTTTT
	817_R	AGGTCCACAGCAAAGATAGGAA	4,360_R	TGTGTGCAAGCTCGTTAAGC
	817_F	TTCCTATCTTTGCTGTGGACCT	5,030_F	CCGGTTGTTGGACATAACTAGG
	997_R	GAATCGCAATCGATAACCAGA	5,135_R	CCAAACCCAGACTTAACCAGAC
			5,534_F	TGGTTGTTATTTGGTGGTGTG
			5,649_R	ATCTCCATCTCAGCTTCTGCTC
HY	48_F	CGACAAGTCACCTTCTCCAAA	3,088_F	GGGGCTGCGTTTACATTTTA
	205_R	AGGGGGAACAAATGAAAACC	3,224_R	GTGATAGCGCTGGCTTTGAT
	307_F	GGCGGATCTCTTGTTGTTTC	3,899_F	CTTTTTCATGGGCAGGATCA
	393_R	CTTCTTCACGACATTGTTCTTCC	4,069_R	TGACATTTGATCCCACAAGC
	543_F	CGTGCTCGATGTTGTTGAGT	4,213_F	AGAACAACCGTGCTGCTTTT
	700_R	TCCCGTAAGTGCATTGCATA	4,360_R	TGTGTGCAAGCTCGTTAAGC
	1,035_F	CCTTTTGCTGTACATAAACTGGTC	5,030_F	CCGGTTGTTGGACATAACTAGG
	1,148_R	CCAAACTTCTTGATCCTTTTTACC	5,135_R	CCAAACCCAGACTTAACCAGAC
			5,534_F	TGGTTGTTATTTGGTGGTGTG
			5,649_R	ATCTCCATCTCAGCTTCTGCTC
JQa	48_F	CGACAAGTCACCTTCTCCAAA	—	—
	205_R	AGGGGGAACAAATGAAAACC		
	307_F	GGCGGATCTCTTGTTGTTTC		
	393_R	CTTCTTCACGACATTGTTCTTCC		
	679_F	TCATTGGATCTCTCGGATTTG		
	817_R	AGGTCCACAGCAAAGATAGGAA		
	1,035_F	CCTTTTGCTGTACATAAACTGGT		
	1,148_R	CCAAACTTCTTGATCCTTTTTACC		
JQb	48_F	CGACAAGTCACCTTCTCCAAA	—	—
	205_R	AGGGGGAACAAATGAAAACC		
	307_F	GGCGGATCTCTTGTTGTTTC		
	393_R	CTTCTTCACGACATTGTTCTTCC		
	543_F	CGTGCTCGATGTTGTTGAGT		
	700_R	TCCCGTAAGTGCATTGCATA		
	1,035_F	CCTTTTGCTGTACATAAACTGGTC		
	1,148_R	CCAAACTTCTTGATCCTTTTTACC		
JQc	48_F	CGACAAGTCACCTTCTCCAAA	—	—
	205_R	AGGGGGAACAAATGAAAACC		
	307_F	GGCGGATCTCTTGTTGTTTC		
	393_R	CTTCTTCACGACATTGTTCTTCC		
	679_F	TCATTGGATCTCTCGGATTTG		
	817_R	AGGTCCACAGCAAAGATAGGAA		
	817_F	TTCCTATCTTTGCTGTGGACCT		
	907_R	GAATCGCAATCGATAACCAGA		

Table S3. Details of the number of ChIP and expression samples taken in each batch

Batch	ChIP samples taken	Relative spliced *FLC* mRNA samples taken
JS	NV: 2	2 wk T7: 5
	2 wk T0: 2	4 wk T7: 5
	4 wk T0: 2	6 wk T7: 7
	6 wk T0: 2	8 wk T7: 2
	8 wk T0: 2	
	2 wk T7: 2	
	4 wk T7: 2	
	6 wk T7: 2	
	8 wk T7: 2	
HY	NV: 3	2 wk T7: 3
	2 wk T0: 3	4 wk T7: 3
	4 wk T0: 3	6 wk T7: 3
	6 wk T0: 3	8 wk T7: 3
	8 wk T0: 3	
	2 wk T7: 3	
	4 wk T7: 3	
	6 wk T7: 3	
	8 wk T7: 3	
JQa	NV: 1	4 wk T10: 3
	2 wk T0: 1	8 wk T10: 3
	4 wk T0: 4	
	8 wk T0: 3	
	4 wk T10: 3	
	8 wk T10: 2	
JQb	NV: 1	
	2 wk T0: 1	
JQc	2 wk T10: 1	